Electronic Supplementary Information (ESI) for:

Preparation and Reactivity of Rhodium and Iridium Complexes Containing a Methylborohydride Based Unit Supported by Two 7-Azaindolyl Heterocycles,

Rosenildo Correa Da Costa, Ben W. Rawe, Nikolaos Tsoureas, Mairi F. Haddow, Hazel A. Sparkes, Graham J. Tizzard, Simon J. Coles and Gareth R. Owen,*

Contents

A. Crystallographic Information for $Li(MeCN)_2[^{Me}Bai]$ and Complexes 1, 2, 3 and 2a.

1. Crystallographic parameters for $Li(MeCN)_2[^{Me}Bai]$ and Complexes **1, 2, 3** and **2a**.

B. Selected Spectroscopy for the Ligand and Complexes

1. Spectra of ligand precursor $Li(NCMe)_2[B(Me)H(azaindolyl)_2]$
   - Figure 1.1 - ^1H NMR spectrum
   - Figure 1.2 - $^1H\{^{11}B\}$ NMR spectrum
   - Figure 1.3 - ^{11}B NMR and $^{11}B\{^1H\}$ spectra
   - Figure 1.4 - $^{13}C\{^1H\}$ NMR spectrum

2. Spectra of complex $[Ir\{\kappa^3\text{-}N,N,H\text{-}B(Me)H(azaindolyl)_2\}(COD)]$ (**1**)
   - Figure 2.1 - ^1H NMR spectrum
   - Figure 2.2 - $^1H\{^{11}B\}$ NMR spectrum
   - Figure 2.3 - ^{11}B NMR and $^{11}B\{^1H\}$ spectra
   - Figure 2.4 - $^{13}C\{^1H\}$ NMR spectrum

3. Spectra of complex $[Rh\{\kappa^3\text{-}N,N,H\text{-}B(Me)H(azaindolyl)_2\}(COD)]$ (**2**)
   - Figure 3.1 - ^1H NMR spectrum
   - Figure 3.2 - $^1H\{^{11}B\}$ NMR spectrum
   - Figure 3.3 - ^{11}B and $^{11}B\{^1H\}$ NMR spectra
   - Figure 3.4 - $^{13}C\{^1H\}$ NMR spectrum

4. Spectra of complex $[Rh\{\kappa^3\text{-}N,N,H\text{-}B(Me)H(azaindolyl)_2\}(COD^{Me})]$ (**2-Me**)
   - Figure 4.1 - ^1H NMR spectrum
   - Figure 4.2 - $^1H\{^{11}B\}$ NMR spectrum
   - Figure 4.3 - ^{11}B and $^{11}B\{^1H\}$ NMR spectra
   - Figure 4.4 - $^{13}C\{^1H\}$ NMR spectrum

5. Spectra of complex $[Rh\{\kappa^3\text{-}N,N,H\text{-}B(Me)H(azaindolyl)_2\}(NBD)]$ (**3**)
   - Figure 5.1 - ^1H NMR spectrum
   - Figure 5.2 - $^1H\{^{11}B\}$ NMR spectrum
   - Figure 5.3 - ^{11}B and $^{11}B\{^1H\}$ NMR spectra
   - Figure 5.4 - $^{13}C\{^1H\}$ NMR spectrum

6. Activation studies of complex $[Rh\{\kappa^3\text{-}N,N,H\text{-}B(Me)H(azaindolyl)_2\}(COD)]$ (**2**) to form **2a**
   - Figure 6.1 – ^{11}B NMR and $^{11}B\{^1H\}$ spectra in C_6D_6 (mixture of **2** and **2a**)
   - Figure 6.2 - ^{11}B NMR and $^{11}B\{^1H\}$ NMR spectra in CD_2Cl_2 (mixture of **2** and **2a**)
   - Figure 6.3 - ^1H NMR spectrum (mixture of **2** and **2a**)
   - Figure 6.4 - Partial $^1H\{^{11}B\}$ NMR spectrum (mixture of **2** and **2a**)
   - Figure 6.5 - ^{11}B NMR and $^{11}B\{^1H\}$ NMR spectra (activated product **2a** – after crystallisation)
   - Figure 6.6 - ^1H NMR spectrum (activated product **2a** – after crystallisation)
   - Figure 6.7 - $^{13}C\{^1H\}$ NMR spectrum (activated product **2a** – after crystallisation)
   - Figure 6.8 - Comparison of infrared of starting complex **2** and product with **2a**

A. Crystallographic Information for Li[^{Me}Bai] and Complexes 1, 2, 3 and 2a.

1. Crystallographic parameters for Li[^{Me}Bai] and Complexes 1, 2, 3 and 2a.

Complex	**Li(NCMe)$_2$[^{Me}Bai]**	**1**	**2**	**3**	**2a**
Formula	$C_{19}H_{20}BLiN_6$	$C_{23}H_{26}BN_4Ir$	$C_{23}H_{26}BN_4Rh$	$C_{22}H_{22}BN_4Rh$	$C_{23}H_{26}BN_4Rh$
$D_{calc.}$/ g cm^{-3}	1.228	1.781	1.502	1.604	1.553
μ/mm^{-1}	0.076	6.393	0.834	0.919	0.863
Formula Weight	350.16	561.49	472.20	456.15	472.20
Colour	colourless	yellow	yellow	yellow	colourless
Size/mm^3	0.49 × 0.36 × 0.12	0.05 × 0.05 × 0.04	0.18 × 0.12 × 0.05	0.50 × 0.10 × 0.10	0.10×0.09×0.08
T/K	100(2)	100(2)	100(2)	100(2)	100(2)
Crystal System	monoclinic	trigonal	triclinic	monoclinic	monoclinic
Space Group	$P2_1/n$	R-3	P-1	C2/c	$P2_1/n$
a/Å	8.3408(4)	26.9680(16)	14.9965(3)	22.5002(3)	14.5731(3)
b/Å	15.0529(6)	26.9680(16)	16.0602(3)	10.5702(2)	16.5975(4)
c/Å	15.1212(6)	14.961(2)	16.3753(5)	15.9172(2)	17.2681(3)
α/°	90	90	111.4750(10)	90	90
β/°	94.024(2)	90	107.6280(10)	93.7480(10)	104.767(2)
γ/°	90	120	106.4890(10)	90	90
V/Å^3	1893.84(14)	9423.2(18)	3132.31(13)	3777.52(10)	4038.80(15)
Z	4	18	6	8	8
Z'	1	1	3	1	2
Wavelength/Å	0.71073	0.71073	0.71073	0.71073	0.71075
Radiation type	MoKα	MoKα	MoKα	MoKα	MoKα
Θ_{min}/°	1.911	2.212	1.52	3.628	2.440
Θ_{max}/°	27.44498	25.342	27.531	55.106	27.483
Measured Refl.	17411	18758	87639	32574	46283
Independent Refl.	4351	3824	14384	4364	9257
R_{int}	0.0305	0.1040	0.0327	0.0189	0.0773
Parameters	250	263	787	257	532
Restraints	0	0	0	0	0
Largest Peak	0.29	2.59	1.40	1.22	2.043
Deepest Hole	-0.21	-2.89	-0.80	-0.40	-1.404
GooF	1.045	1.129	1.064	1.032	1.043
wR_2 (all data)	0.0984	0.1283	0.0743	0.0544	0.1559
wR_2	0.0930	0.1165	0.0701	0.0531	0.1407
R_1 (all data)	0.0455	0.1018	0.0362	0.0223	0.0771
R_1	0.0375	0.0661	0.0286	0.0207	0.0571
CCDC Dep. No.	1847347	1847348	1847349	1847350	1847138

B. Selected Spectroscopy for the Ligand and Complexes

1. Spectra for Li(NCMe)$_2$[B(Me)H(azaindolyl)$_2$]

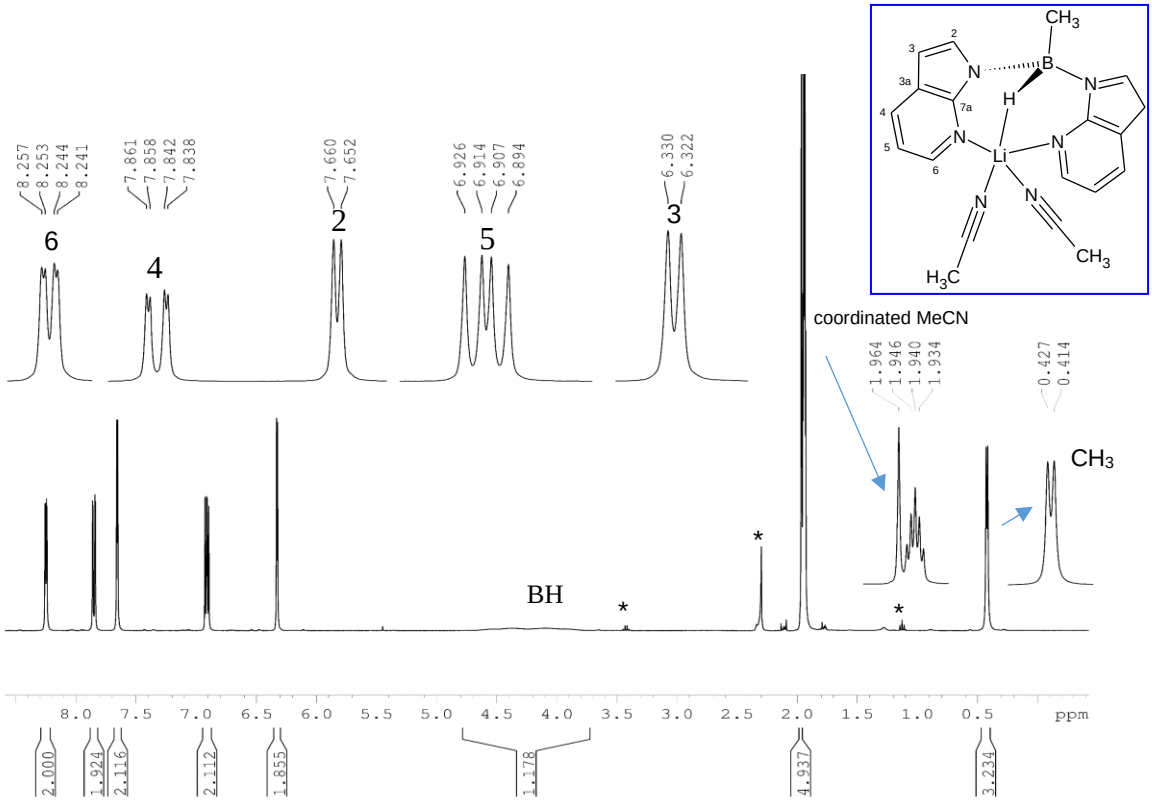

Figure 1.1: ^{1}H NMR (CD_3CN), 400.13 MHz, 298 K (* = residual solvent)

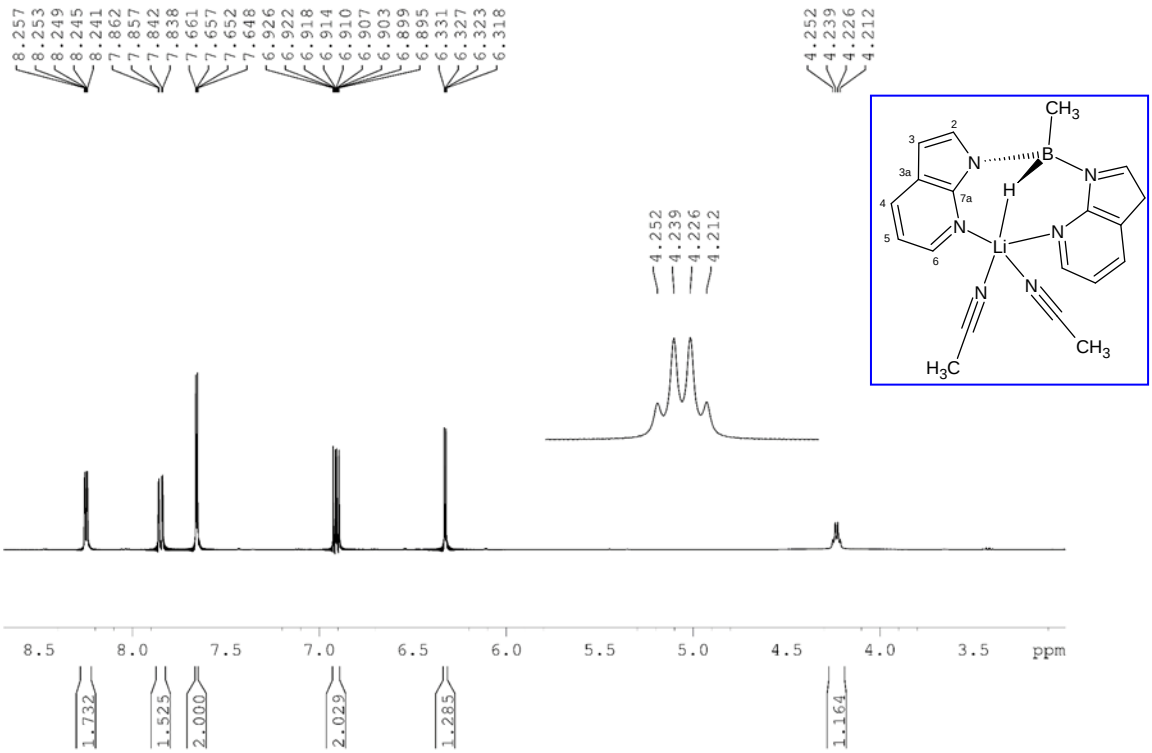

Figure 1.2: Partial ^{1}H{^{11}B} NMR (CD_3CN), 400.13 MHz, 298 K highlighting the BH unit

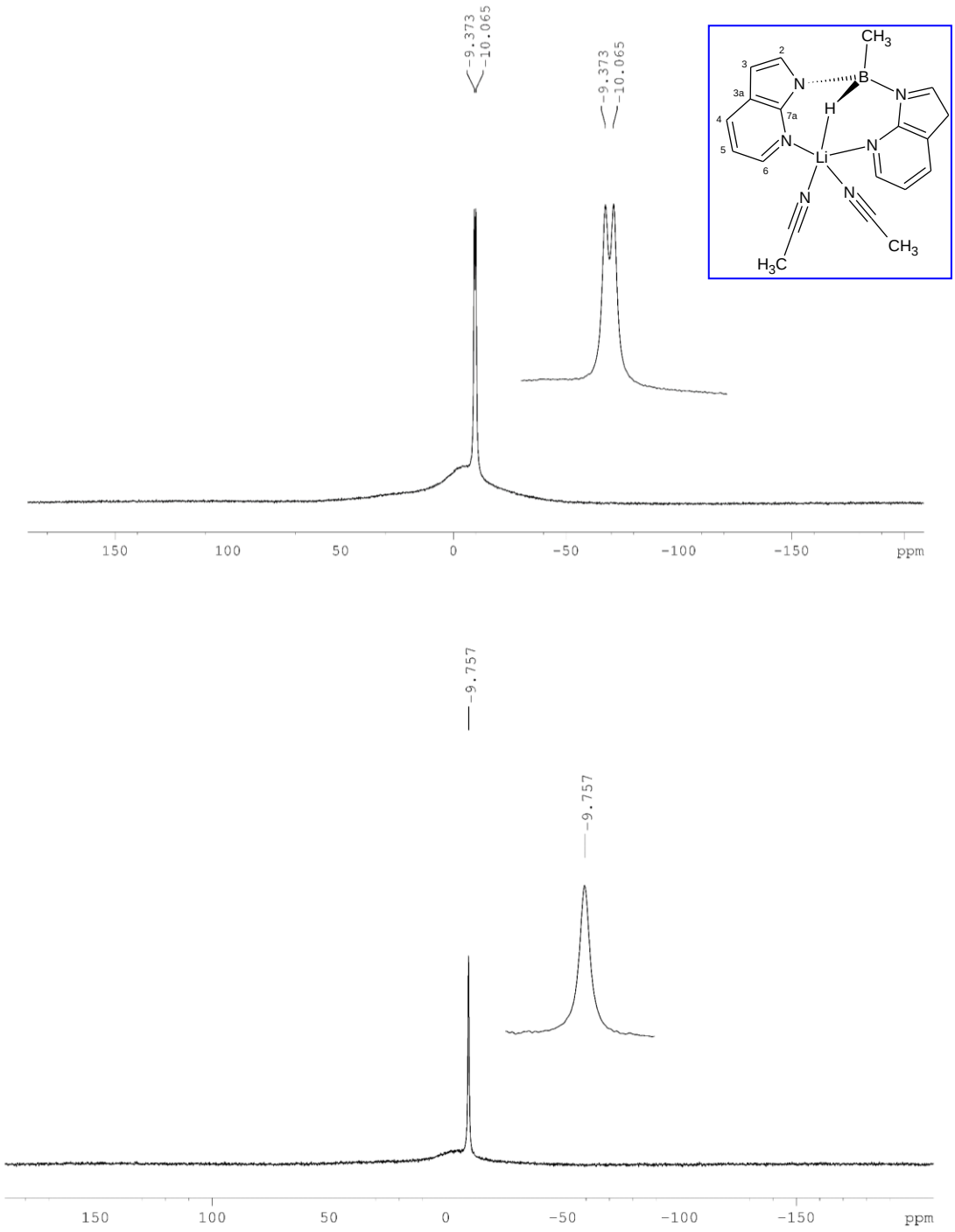

Figure 1.3: ^{11}B NMR (top) and $^{11}B\{^{1}H\}$ (bottom) in CD_3CN, 128.37 MHz, 298 K

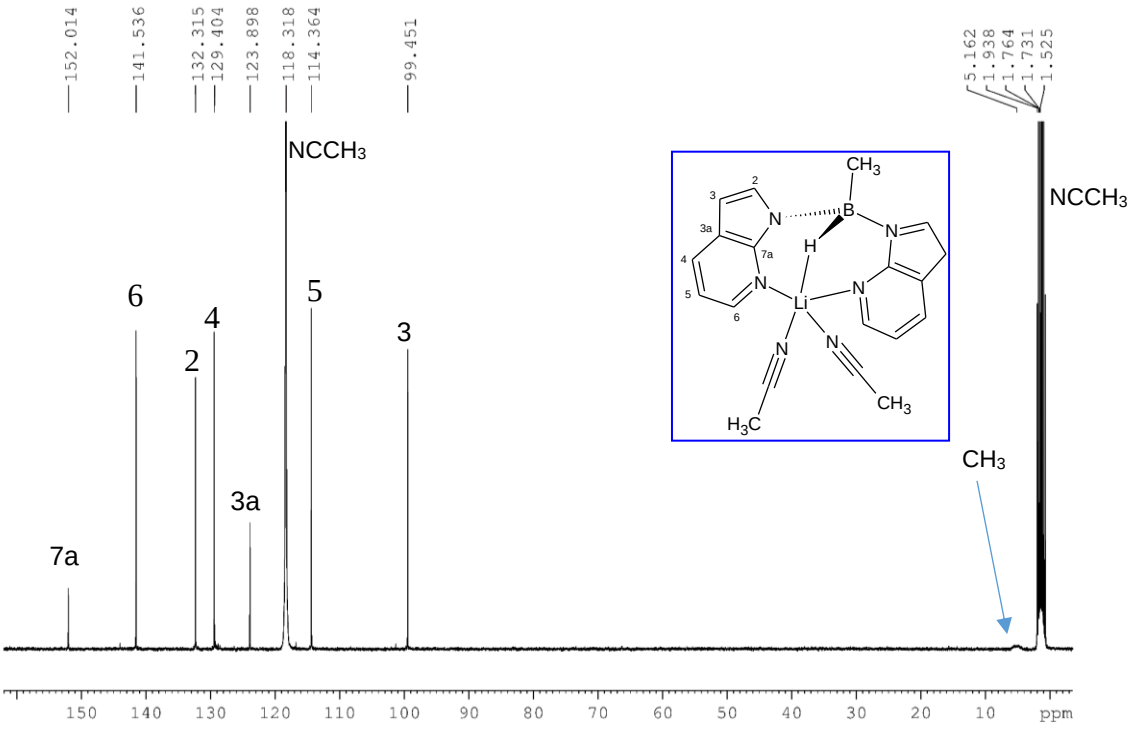

Figure 1.4: $^{13}C\{^{1}H\}$ NMR, CD_3CN, 100.62 MHz, 298 K

2. Spectra of complex [Ir{κ³-*N,N,H*-B(Me)H(azaindolyl)₂}(COD)] (1)

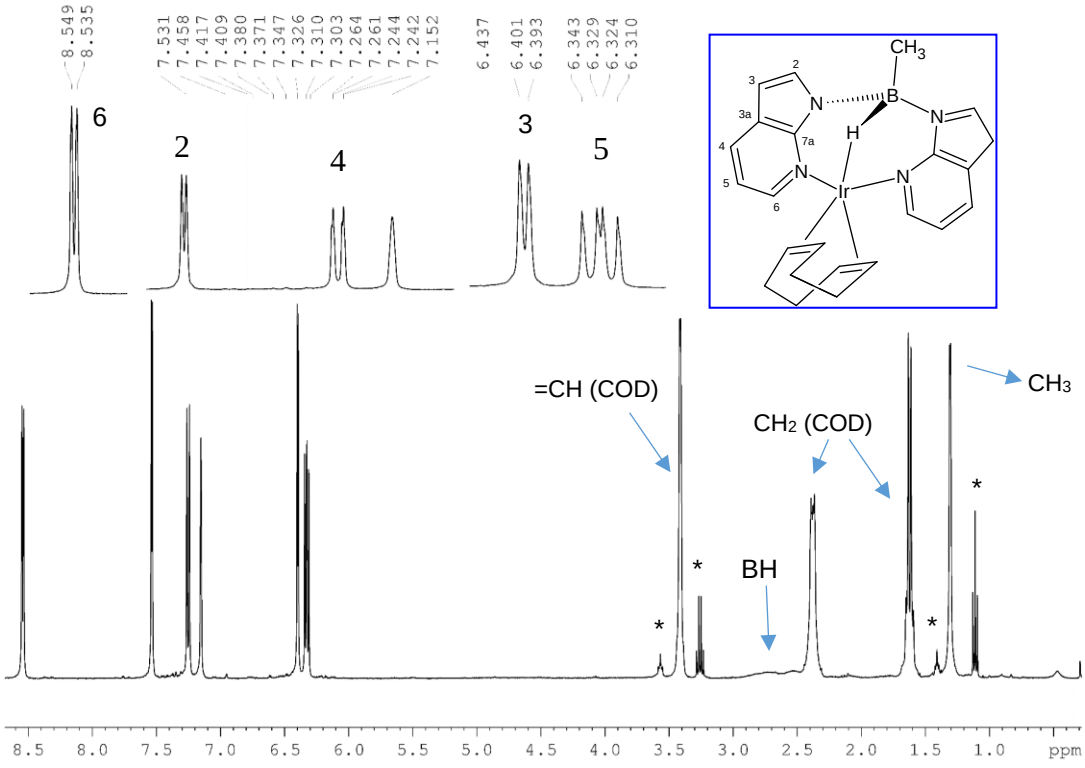

Figure 2.1: ^{1}H NMR (C_6D_6), 400.13 MHz, 298 K (* = residual solvent)

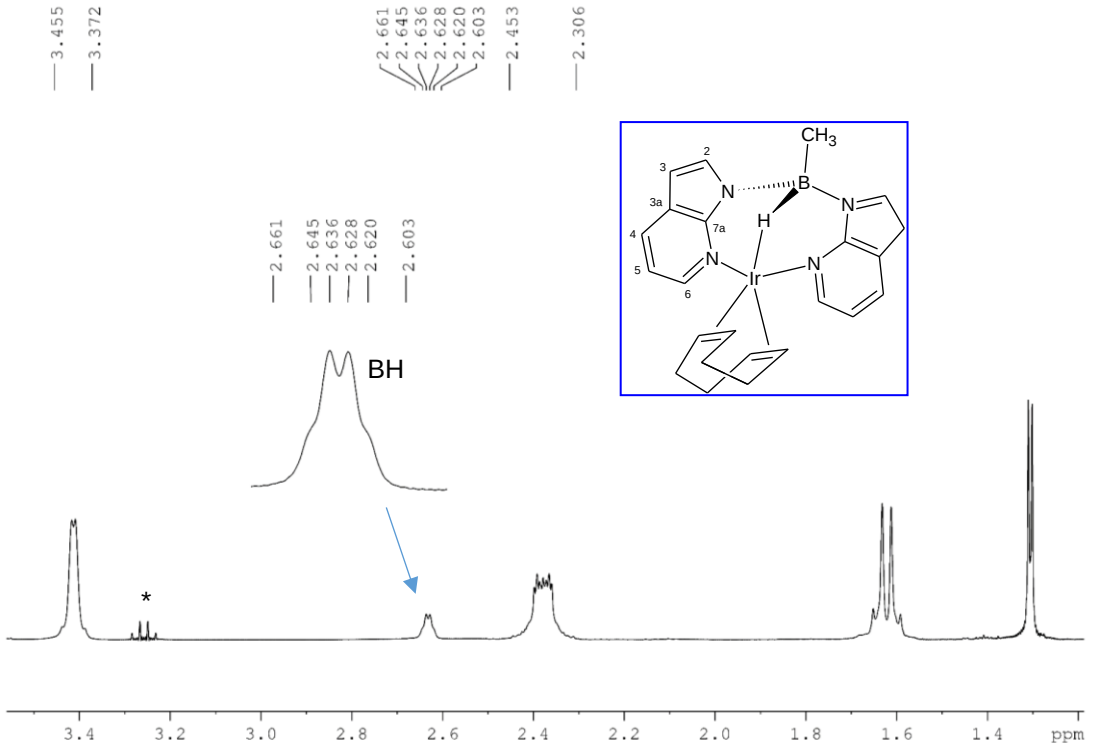

Figure 2.2: Partial $^{1}H\{^{11}B\}$ NMR (C_6D_6), 400.13 MHz, 298 K (* = residual solvent)

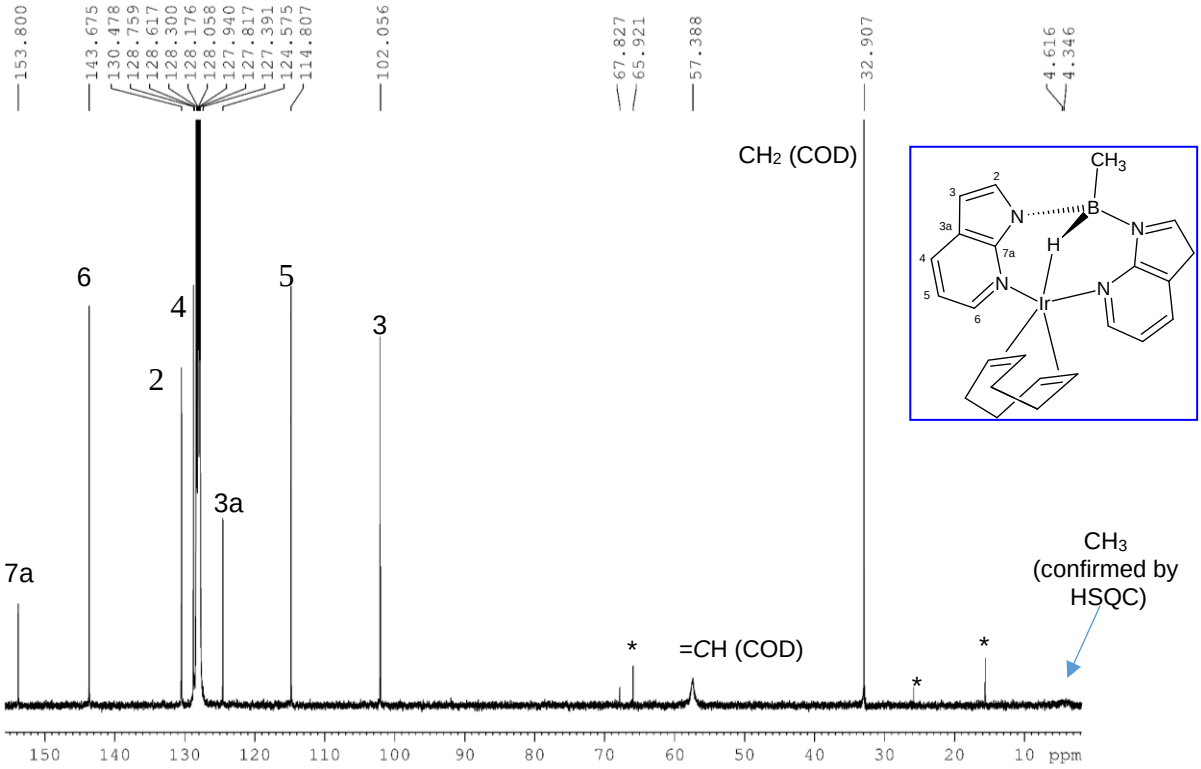

Figure 2.3: $^{13}C\{^{1}H\}$ NMR (C_6D_6), 100.62 MHz, 298 K (* = residual solvent)

3. Spectra of complex [Rh{κ³-*N,N,H*-B(Me)H(azaindolyl)₂}(COD)] (2)

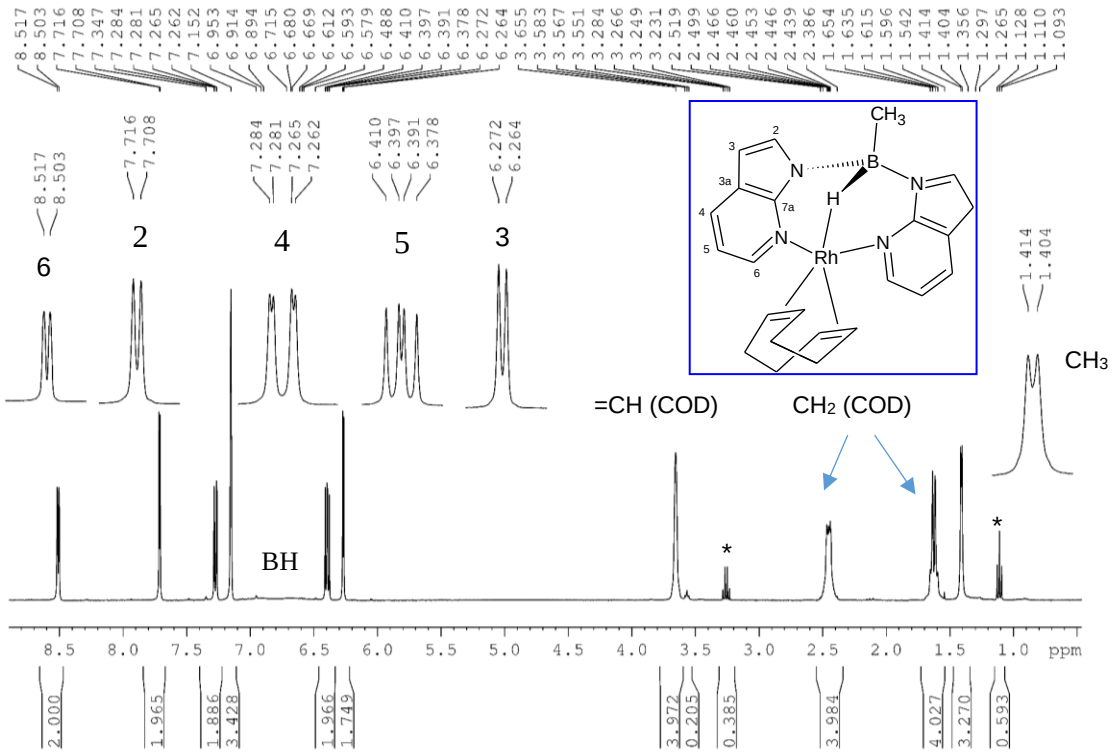

Figure 3.1: ^{1}H NMR, C_6D_6, 400.13 MHz, 298 K (* = residual diethyl ether solvent)

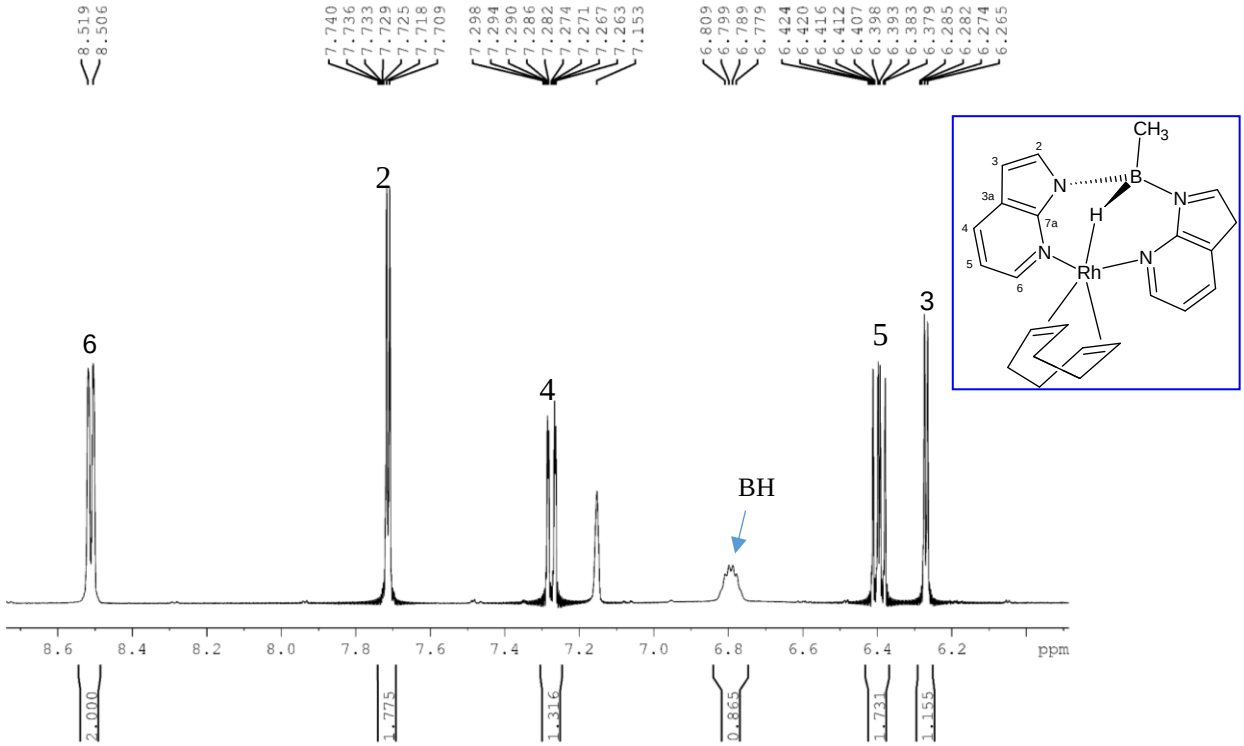

Figure 3.2: Partial $^{1}H\{^{11}B\}$ NMR, C_6D_6, 400.13 MHz, 298 K

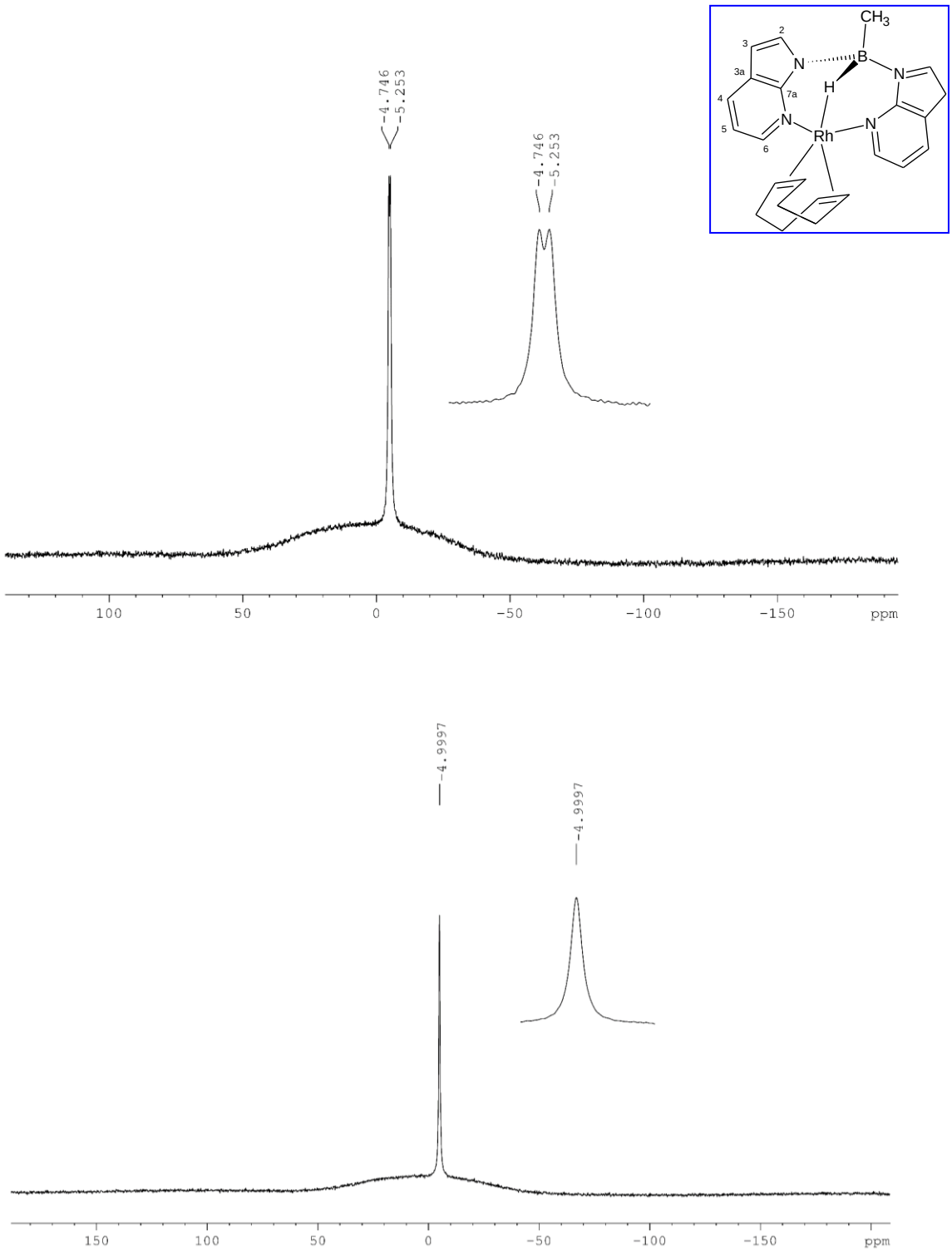

Figure 3.3: ^{11}B NMR (top) and $^{11}B\{^{1}H\}$ (bottom) NMR, C_6D_6, 128.37 MHz, 298 K [Rh{κ^3-*N,N,H*-B(Me)H(azaindolyl)$_2$}(COD)] (**2**)

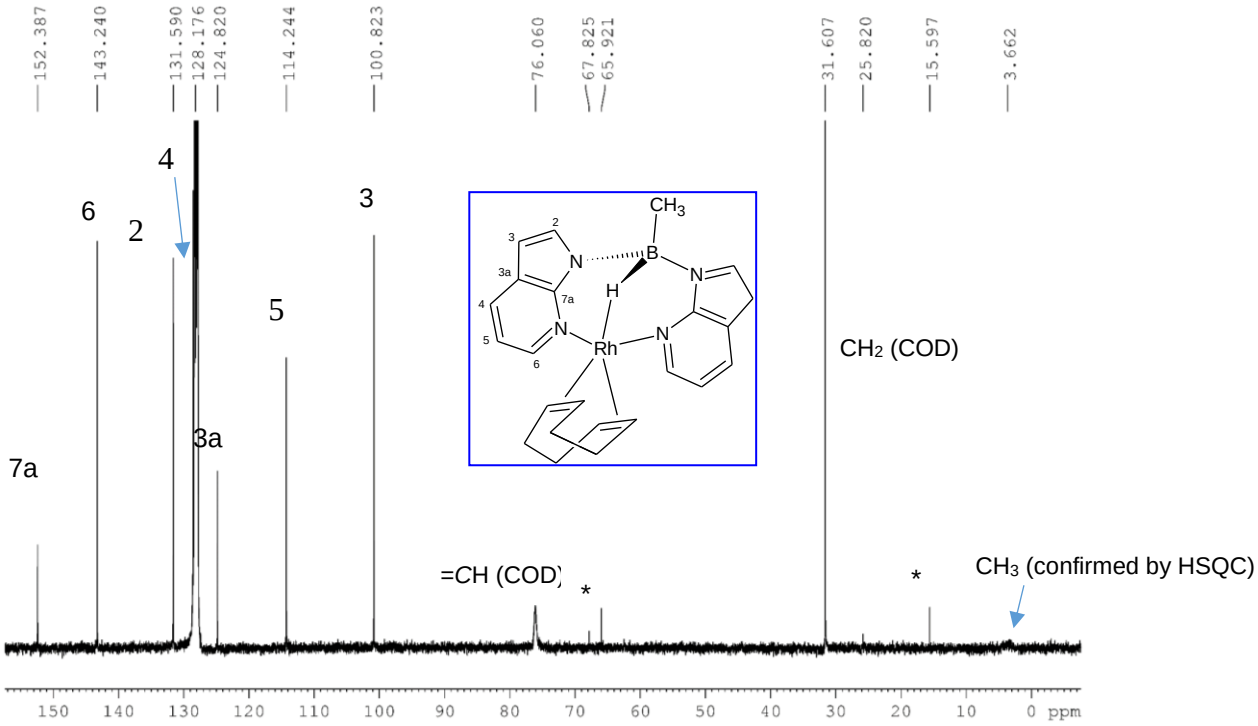

Figure 3.4: $^{13}C\{^{1}H\}$ NMR (C_6D_6), 100.62 MHz, 298 K (* = residual solvent)

4. Spectra of complex [Rh{κ³-*N,N,H*-B(Me)H(azaindolyl)$_2$}(COD^{Me})] (2-Me)

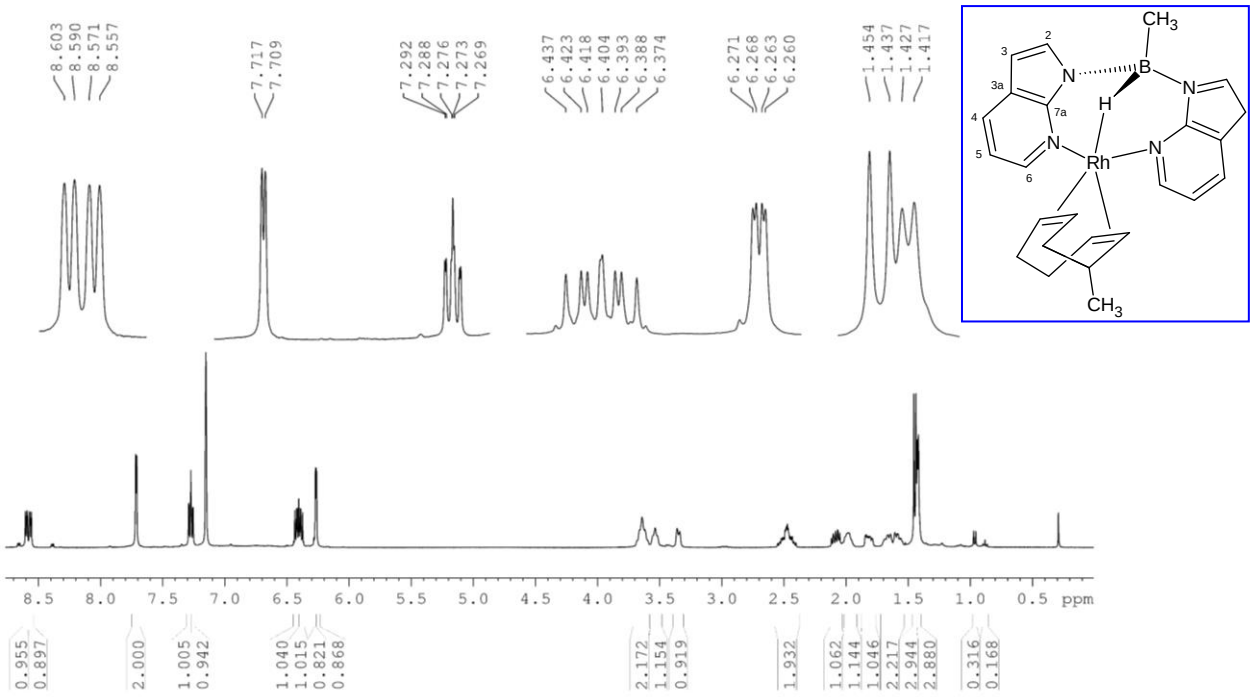

Figure 4.1: ^{1}H NMR, C_6D_6, 400.13 MHz, 298 K:[Rh{κ³-*N,N,H*-B(Me)H(azaindolyl)$_2$}(COD^{Me})] (**2-Me**)

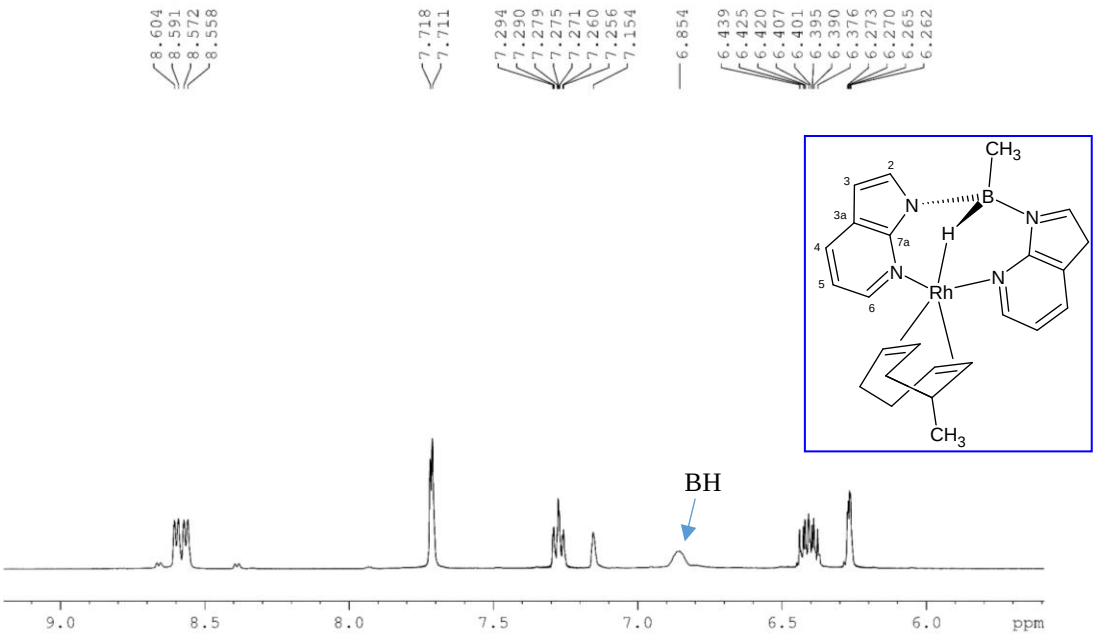

Figure 4.2: Partial $^{1}H\{^{11}B\}$ NMR, C_6D_6, 400.13 MHz, 298 K

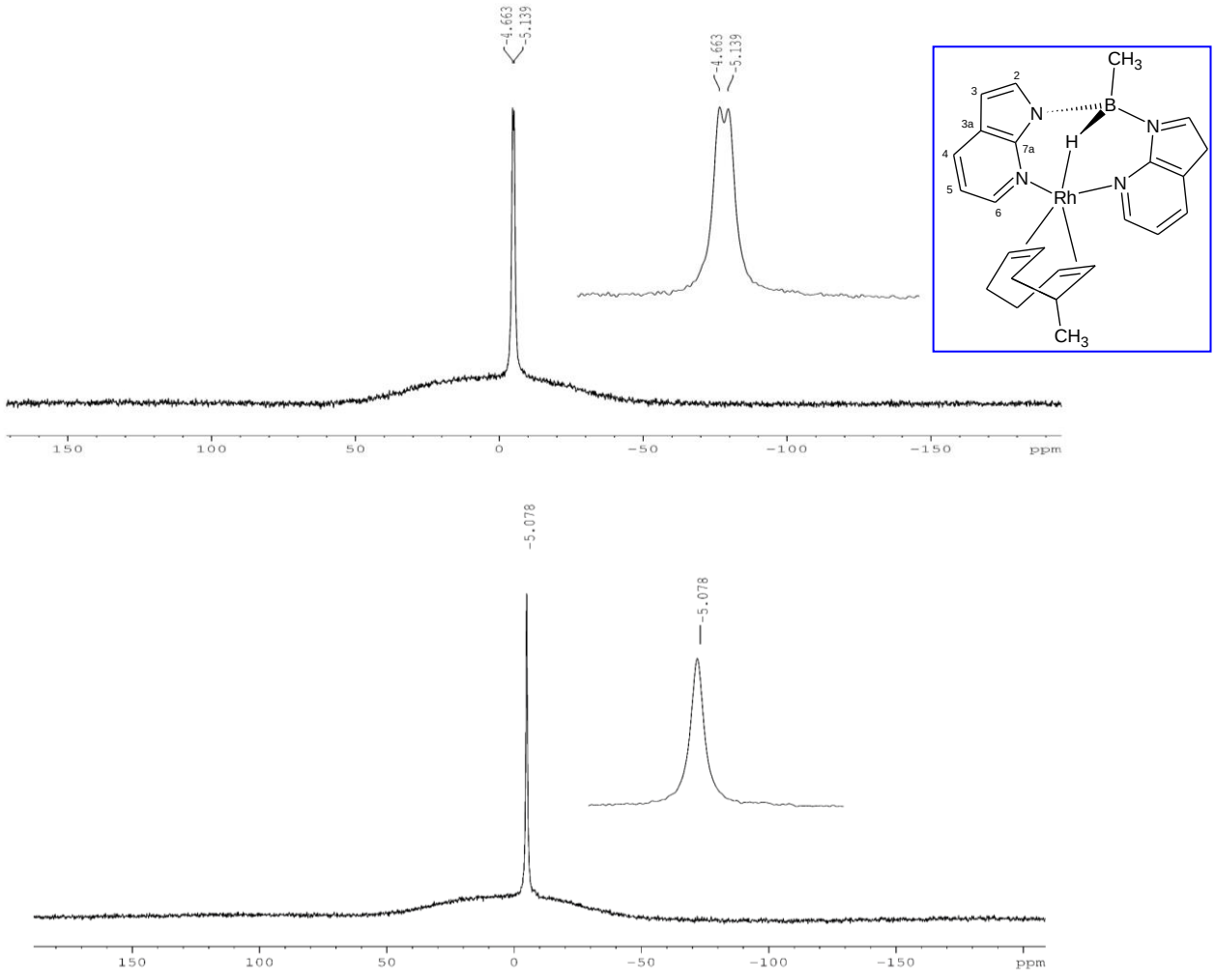

Figure 4.3: ^{11}B NMR (top) and $^{11}B\{^{1}H\}$ (bottom) NMR, C_6D_6, 128.37 MHz, 298 K [Rh{κ^3-*N,N,H*-B(Me)H(azaindolyl)$_2$}(COD)] (**2-Me**)

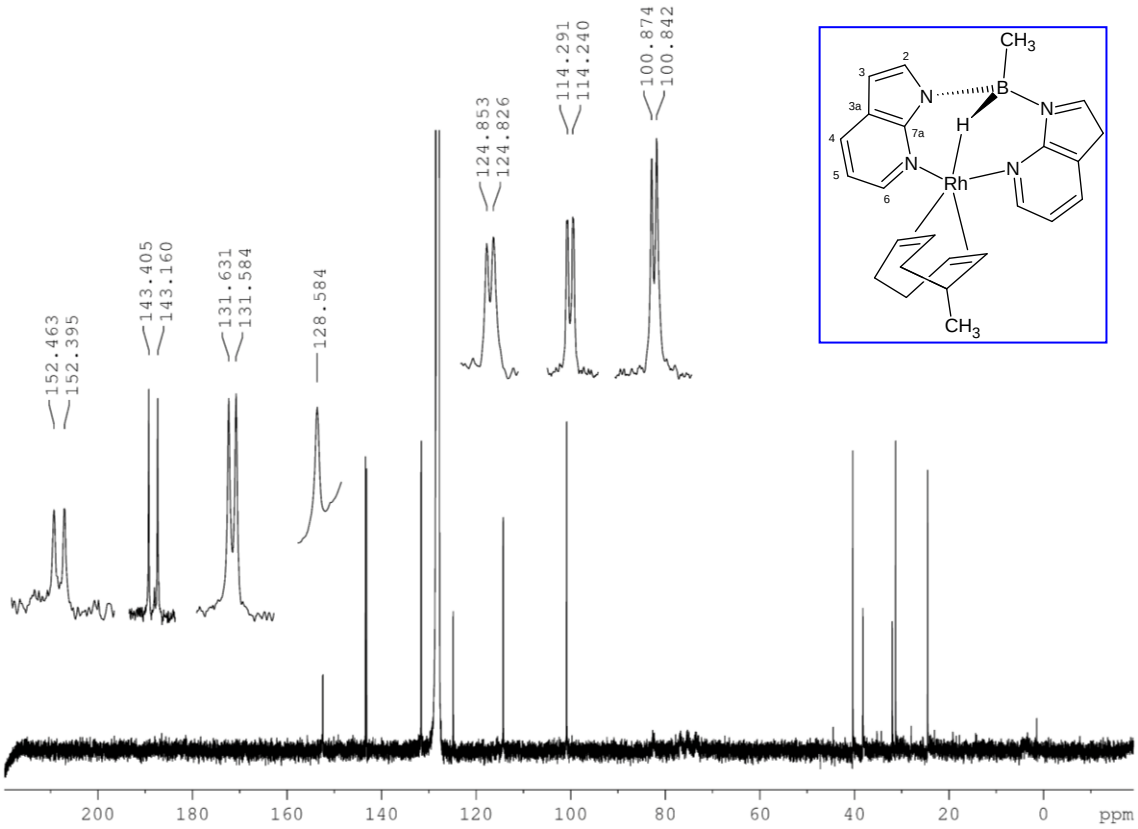

Figure 4.4: $^{13}C\{^{1}H\}$ NMR (C_6D_6), 100.62 MHz, 298 K

5. Spectra of complex [Rh{κ³-*N,N,H*-B(Me)H(azaindolyl)₂}(NBD)] (3)

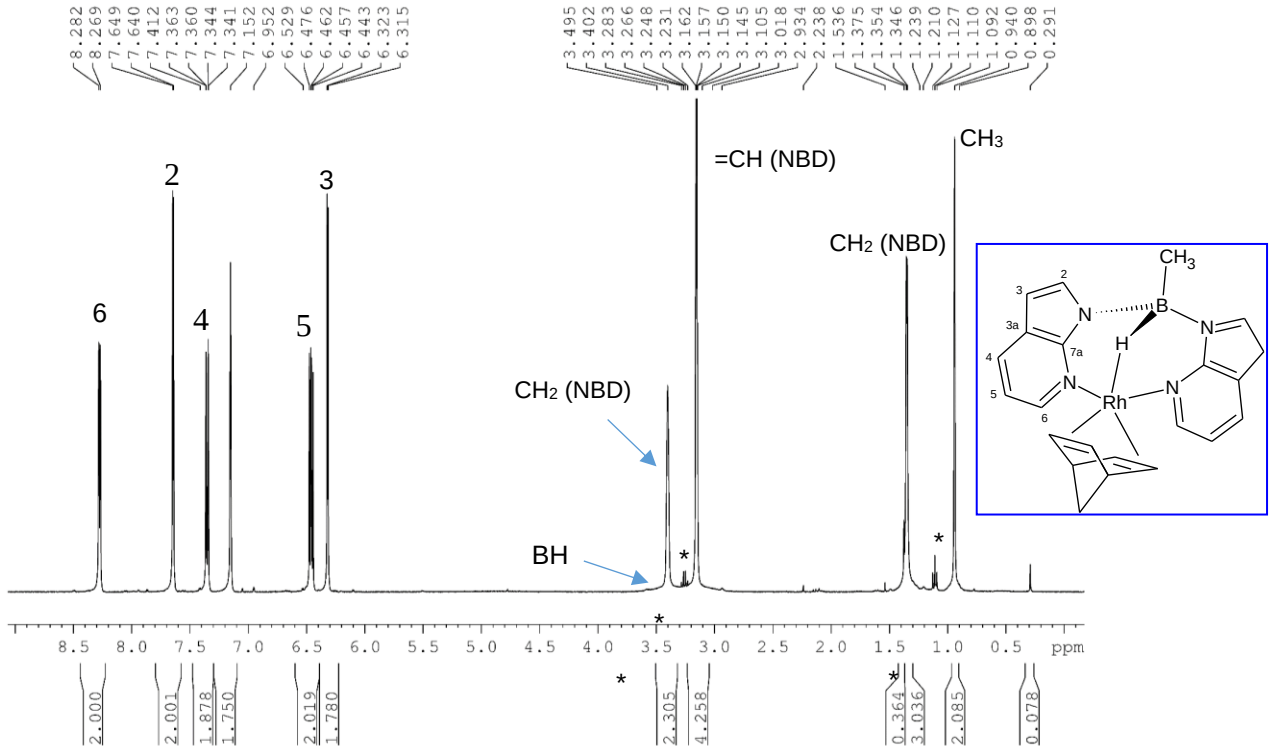

Figure 5.1: ^{1}H NMR (C_6D_6), 400.13 MHz, 298 K (* = residual solvent)

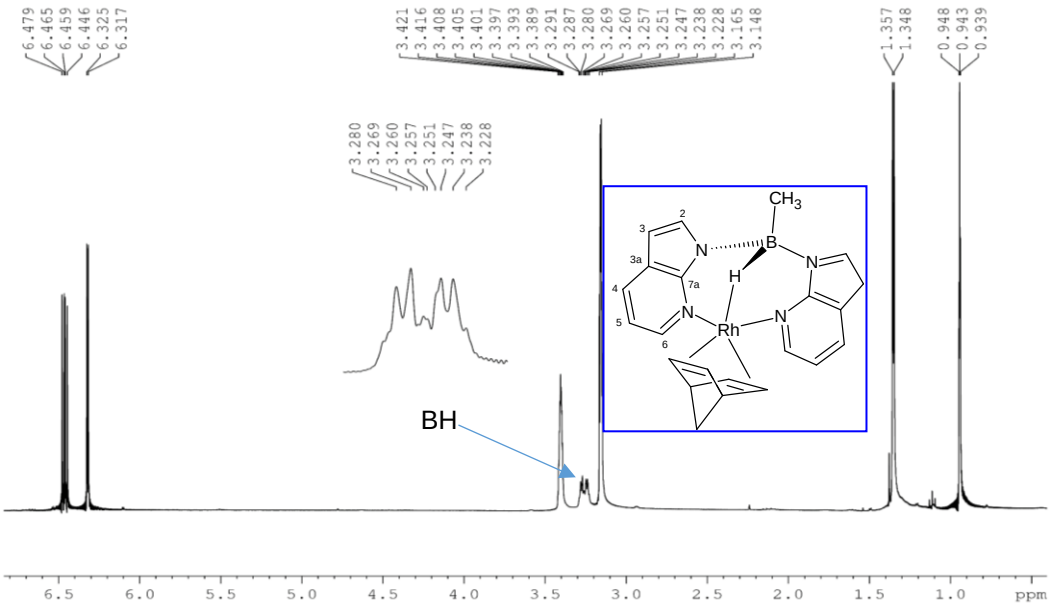

Figure 5.2: Partial $^{1}H\{^{11}B\}$ NMR (C_6D_6), 400.13 MHz, 298 K (* = residual solvent)

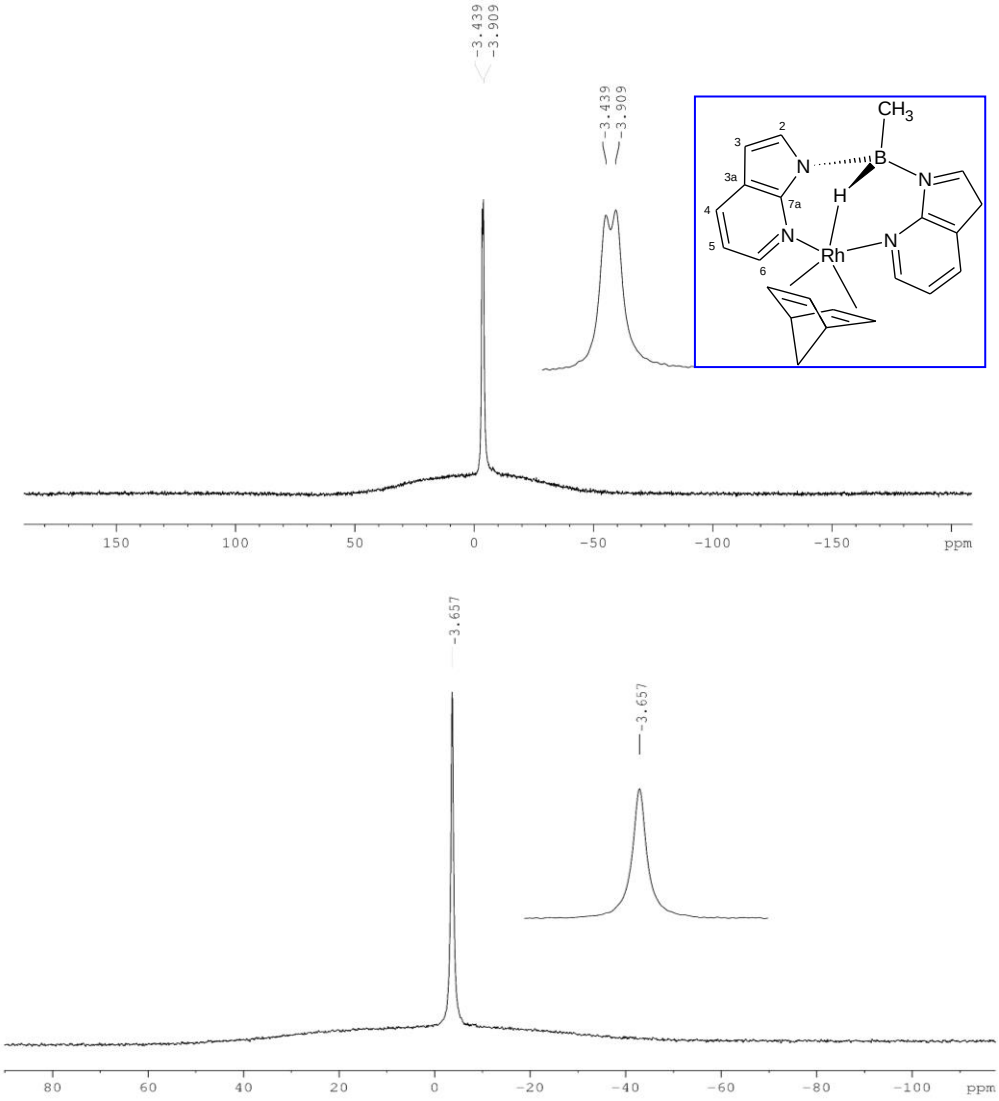

Figure 5.3: ^{11}B NMR (top) and $^{11}B\{^{1}H\}$ (bottom) in CD_3CN, 128.37 MHz, 298 K

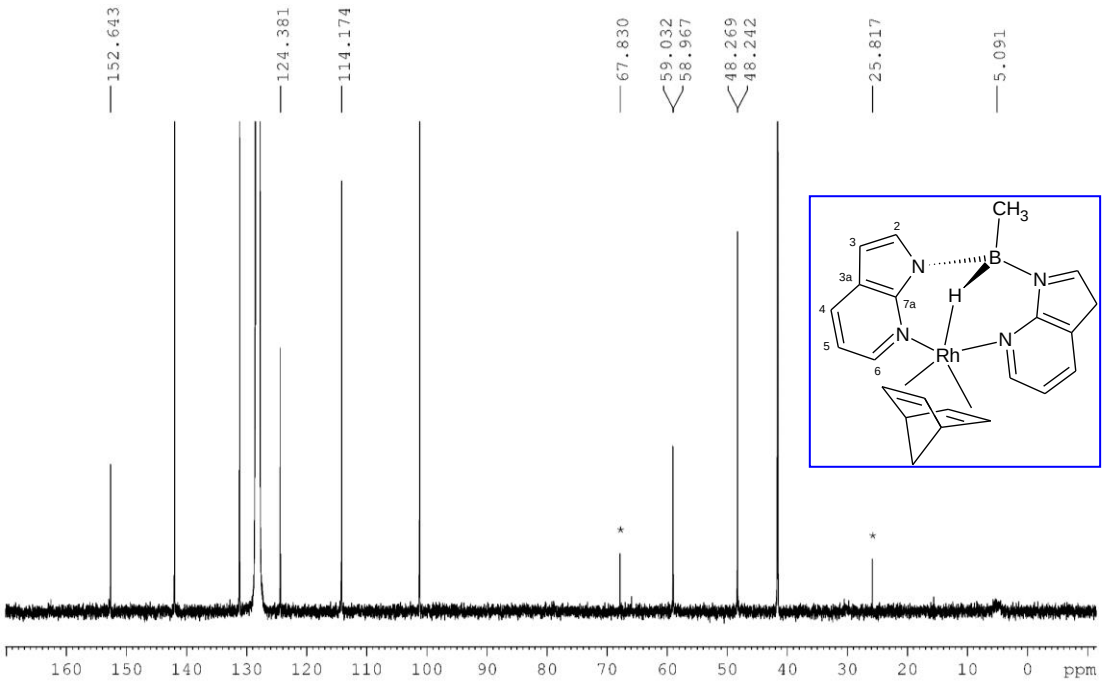

Figure 5.4: $^{13}C\{^{1}H\}$ NMR (C_6D_6), 100.62 MHz, 298 K (* = residual solvent)

6. Activation studies of complex [Rh{κ³-*N,N,H*-B(Me)H(azaindolyl)$_2$}(COD)] (2) to form 2a

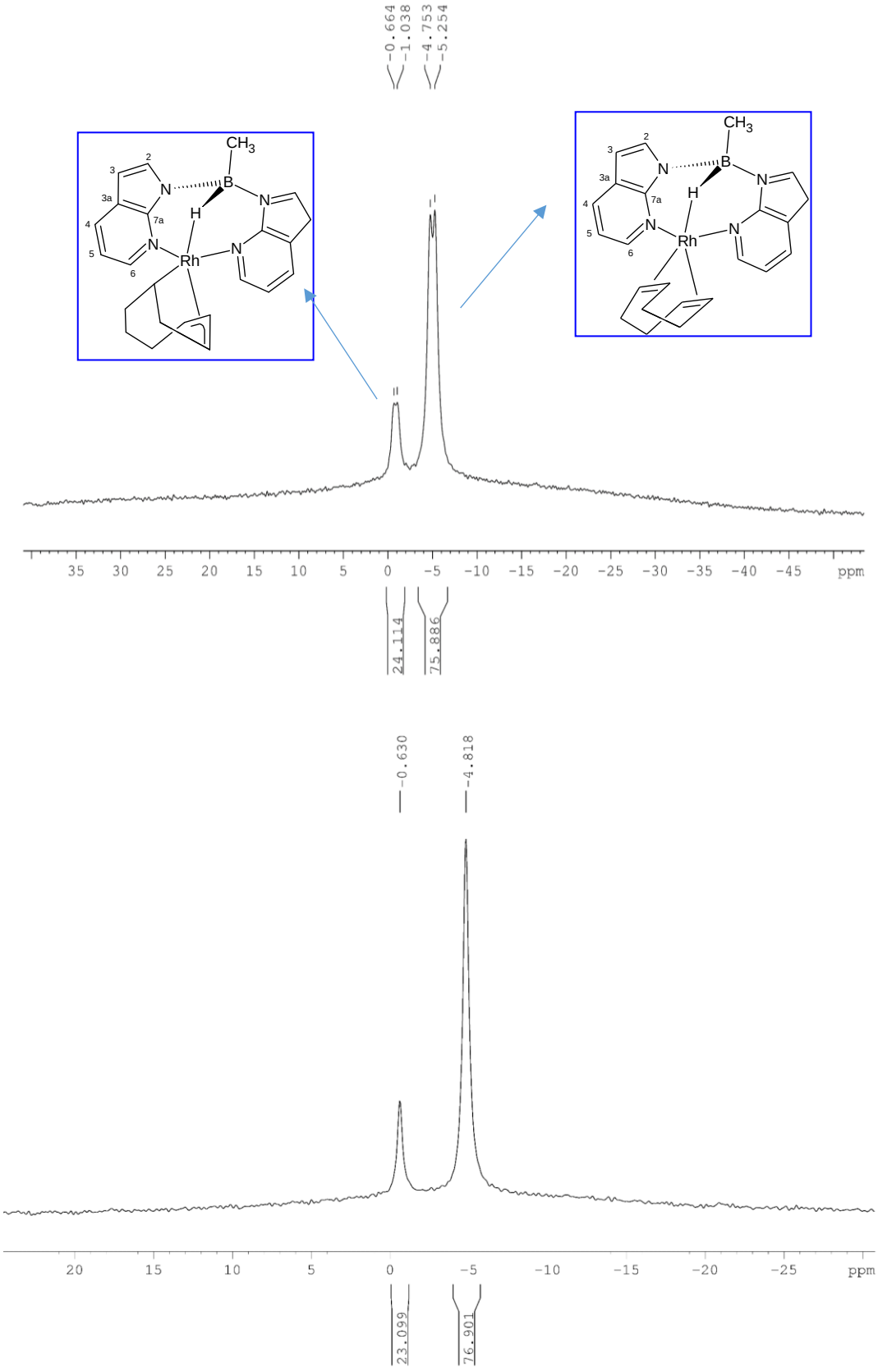

Figure 6.1: ^{11}B NMR (top) and ^{11}B{^{1}H} (bottom) in C_6D_6, 128.37 MHz, 298 K

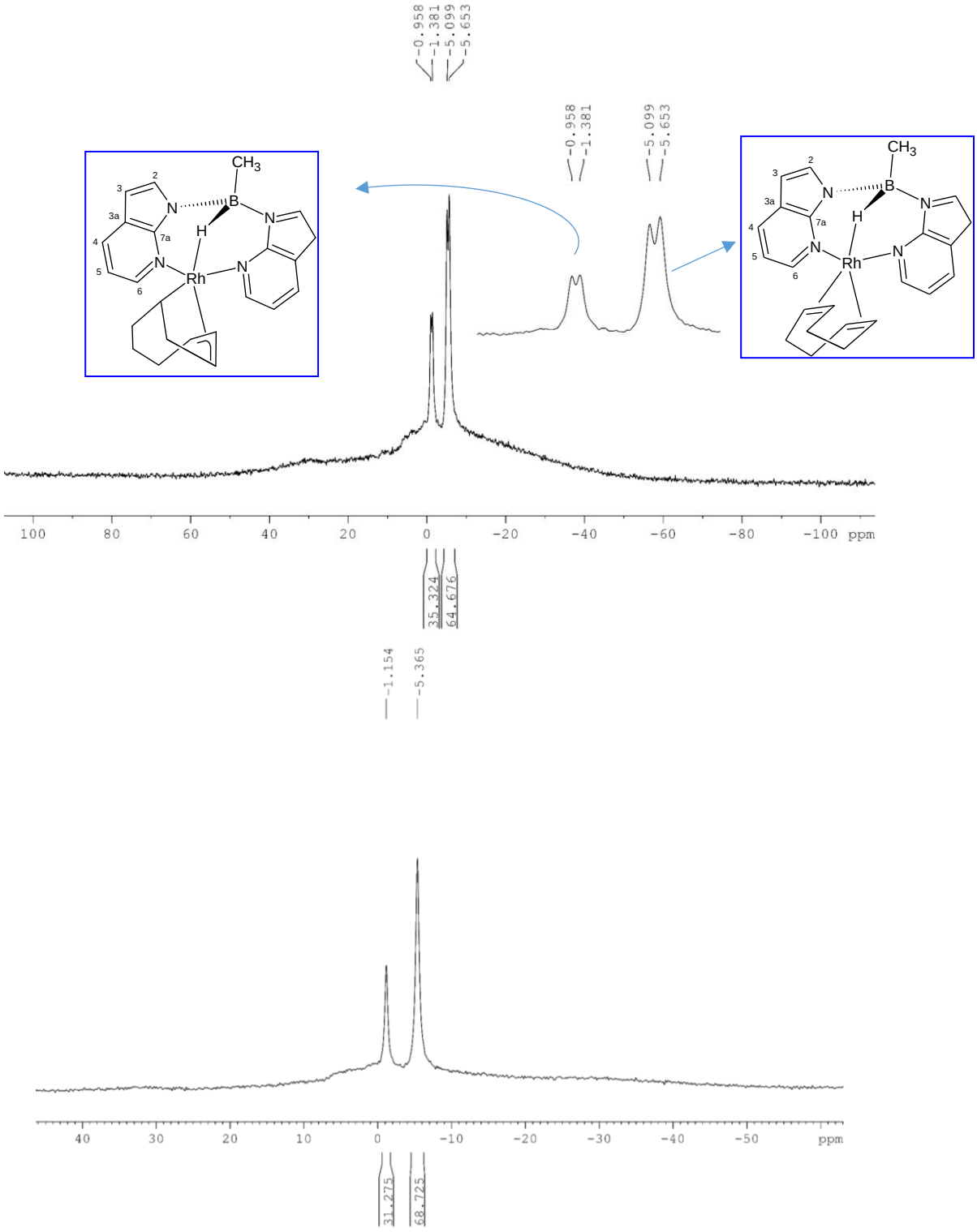

Figure 6.2: ^{11}B NMR (top) and $^{11}B\{^{1}H\}$ (bottom) NMR, 128.37 MHz, 298 K in DCM-d_2

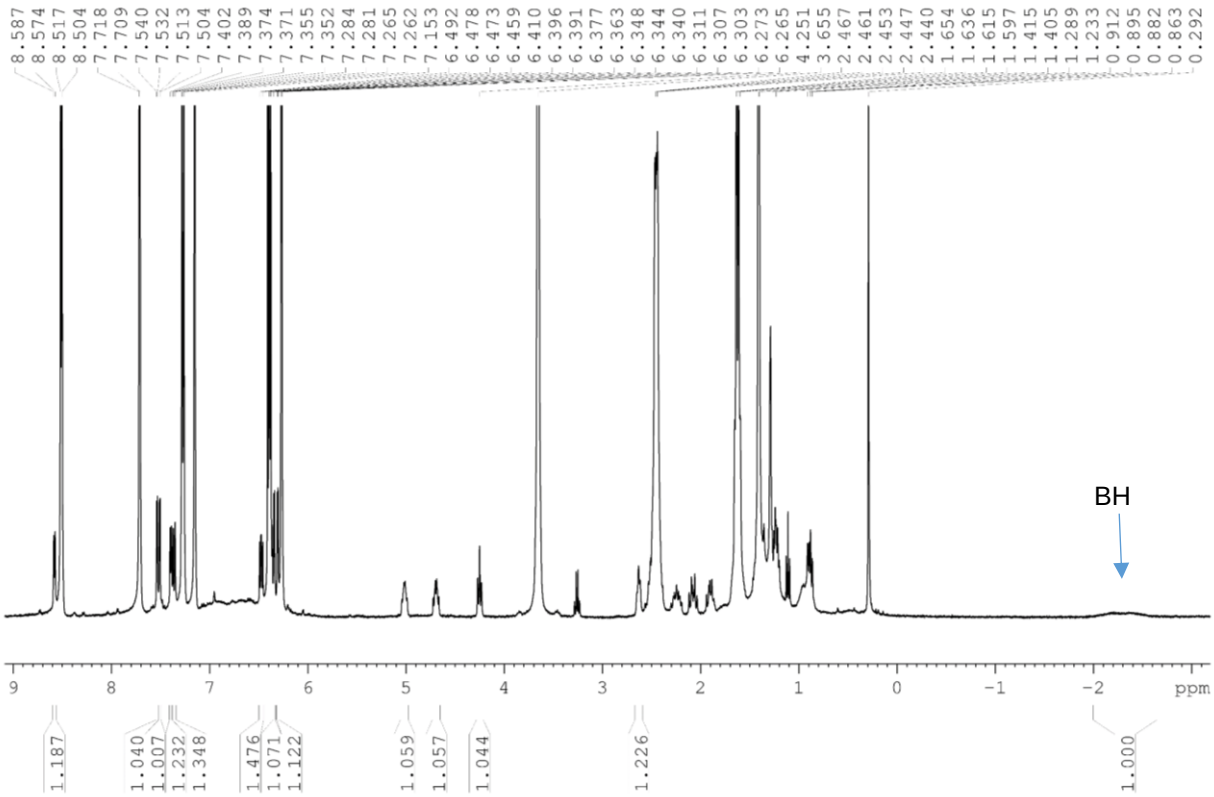

Figure 6.3: ^{1}H NMR, C_6D_6, 400.13 MHz, 298 K

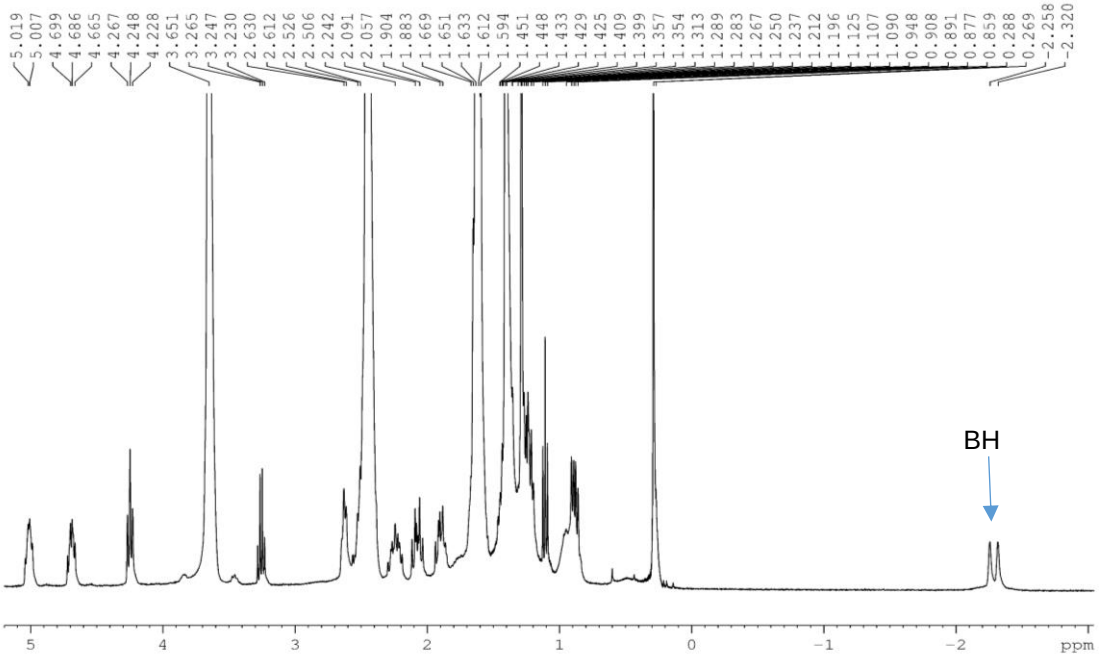

Figure 6.4: Partial $^{1}H\{^{11}B\}$ NMR, C_6D_6, 400.13 MHz, 298.2 K to 238.2 K

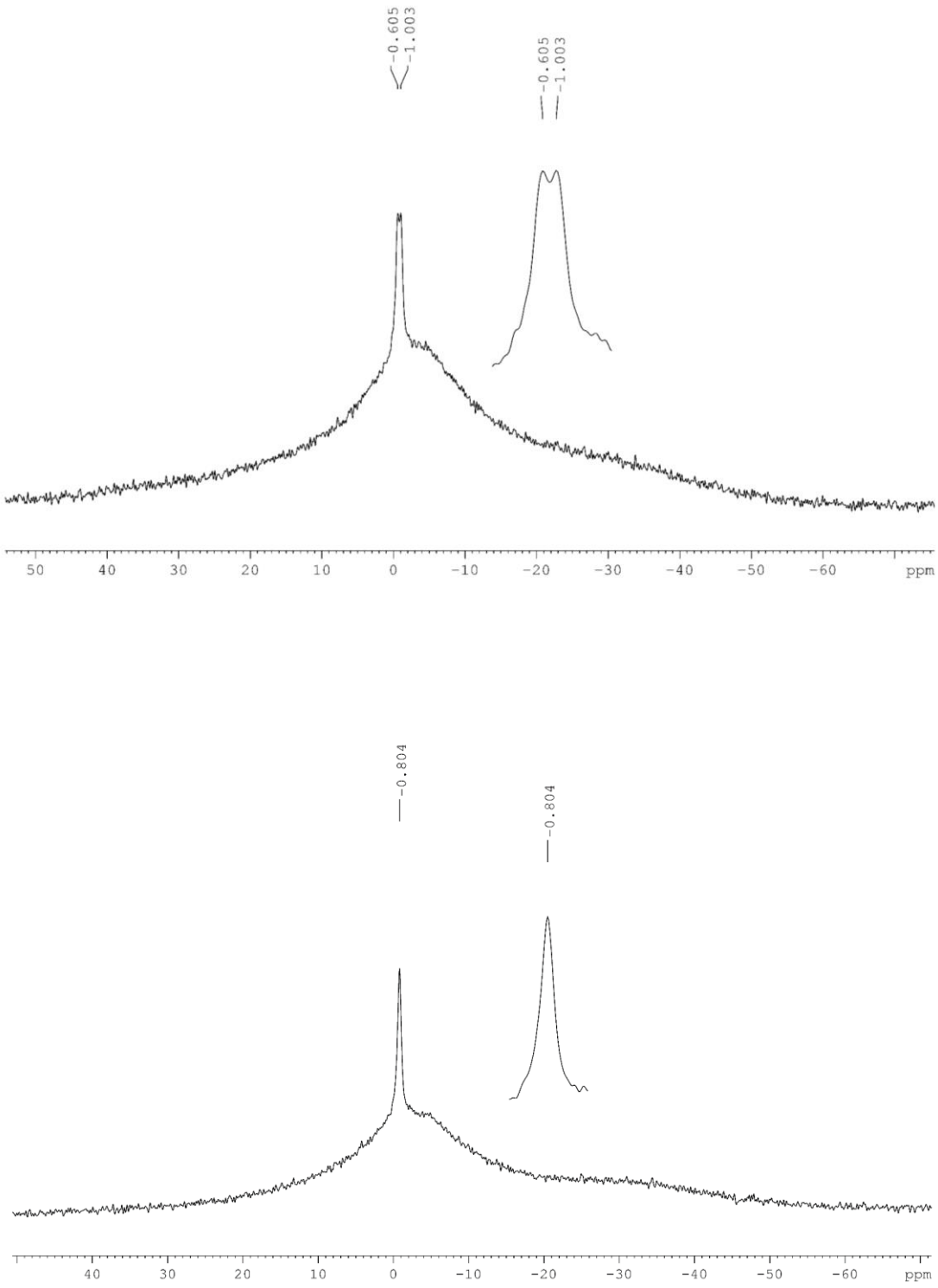

Figure 6.5: ^{11}B NMR (top) and $^{11}B\{^{1}H\}$ (bottom) NMR, C_6D_6, 128.37 MHz, 298 K (activated product **2a** – after crystallisation)

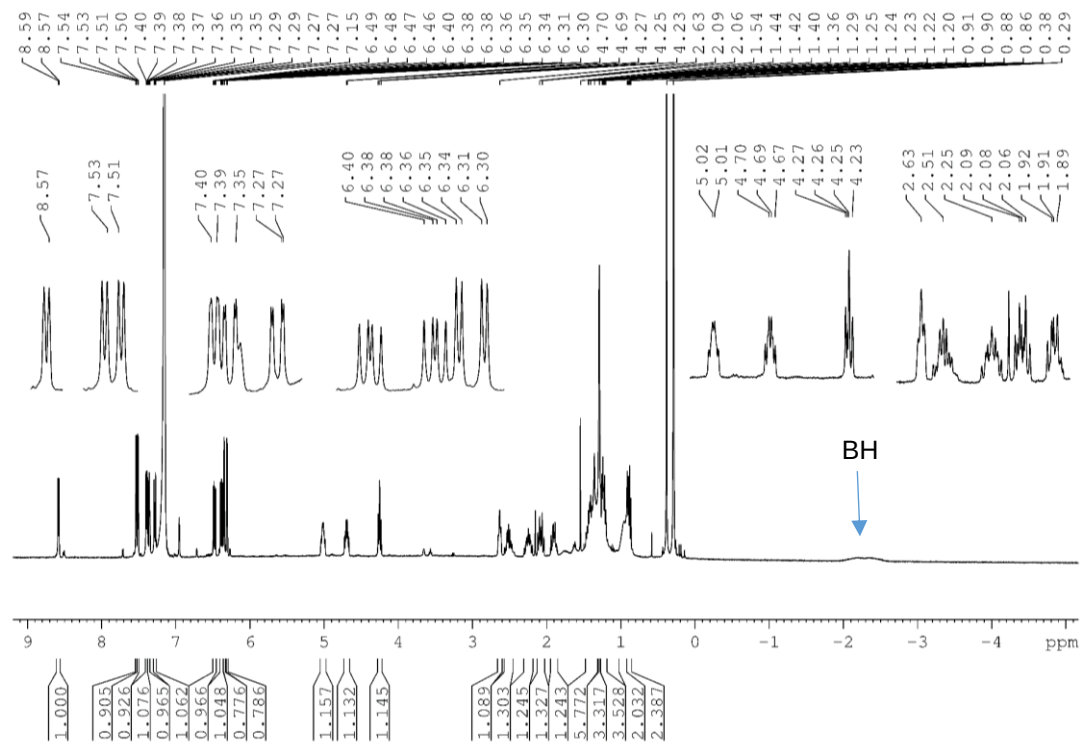

Figure 6.6: ^{1}H NMR, C_6D_6, 400.13 MHz, 298 K (activated product **2a –** after crystallisation)

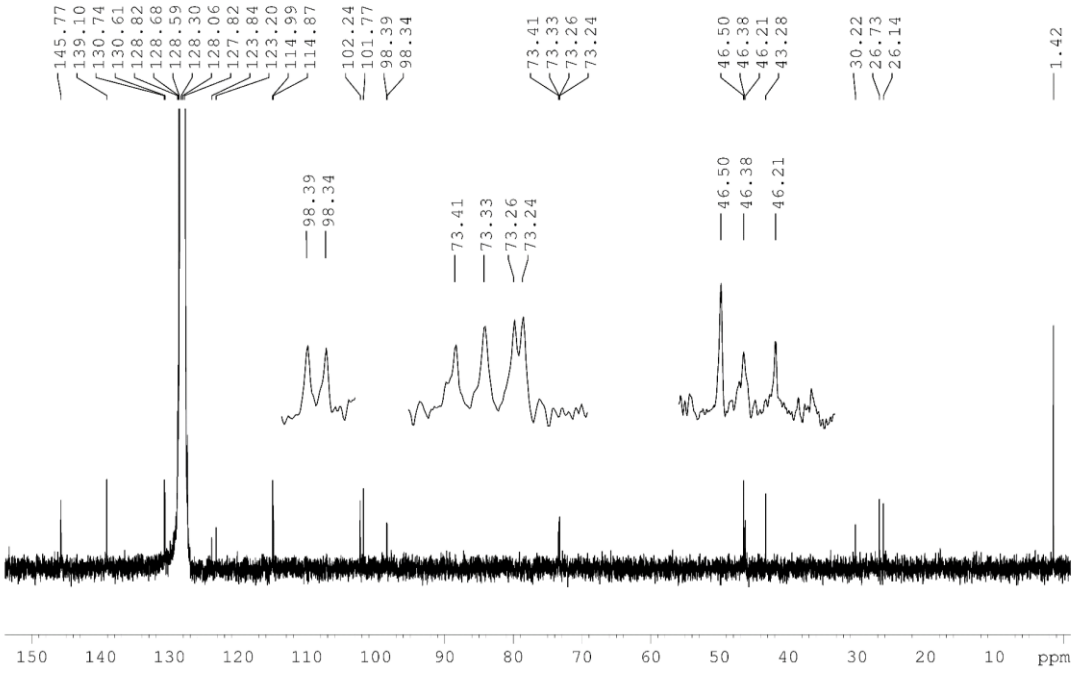

Figure 6.7: $^{13}C\{^{1}H\}$ NMR (C_6D_6), 100.62 MHz, 298 K (activated product **2a -** after crystallisation)

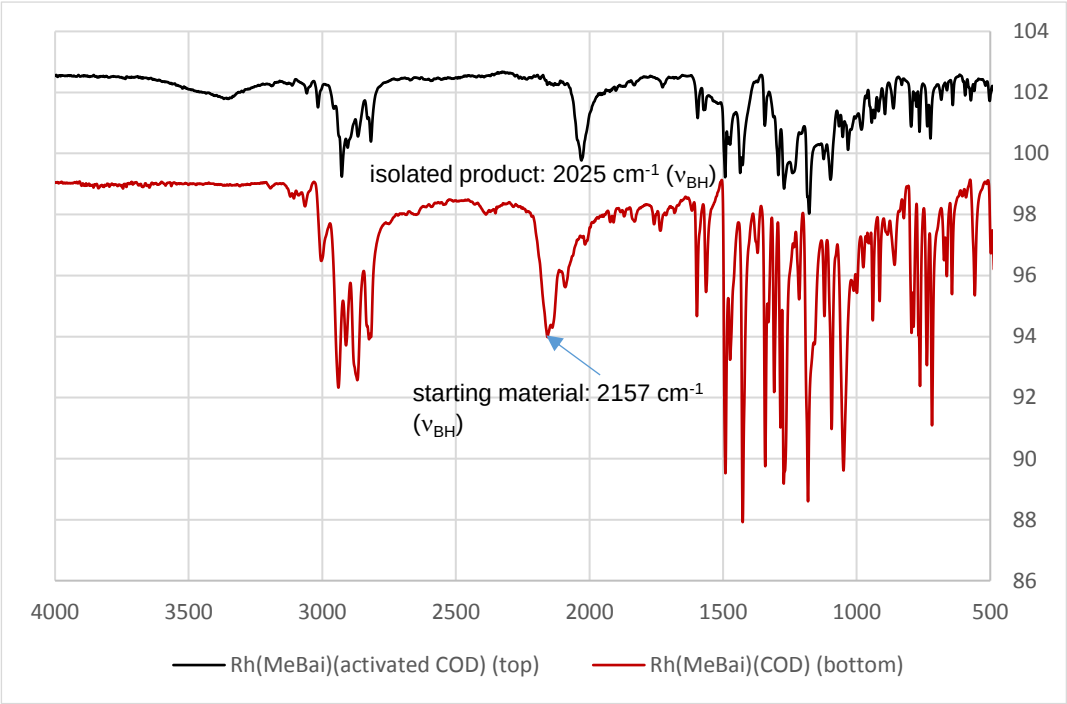

Figure 6.8: Comparison of infrared of starting complex **2** and activated product **2a**